



Full Length Article

Pharmacological inhibition of tankyrase induces bone loss in mice by increasing osteoclastogenesis



Shunichi Fujita^a, Tomoyuki Mukai^{a,*}, Takafumi Mito^a, Shoko Kodama^a, Akiko Nagasu^a, Mizuho Kittaka^b, Teruki Sone^c, Yasuyoshi Ueki^b, Yoshitaka Morita^a

^a Department of Rheumatology, Kawasaki Medical School, Kurashiki, Japan

^b Department of Oral and Craniofacial Sciences, School of Dentistry, University of Missouri-Kansas City, MO, USA

^c Department of Nuclear Medicine, Kawasaki Medical School, Kurashiki, Japan

ARTICLE INFO

Article history:

Received 15 August 2017

Revised 5 October 2017

Accepted 18 October 2017

Available online 18 October 2017

Keywords:

Tankyrase

SH3BP2

Osteoclastogenesis

Osteoblastogenesis

Wnt inhibitor

Tankyrase inhibitor

ABSTRACT

Tankyrase is a poly (ADP-ribose) polymerase that leads to ubiquitination and degradation of target proteins. Since tankyrase inhibitors suppress the degradation of AXIN protein, a negative regulator of the canonical Wnt pathway, they effectively act as Wnt inhibitors. Small molecule tankyrase inhibitors are being investigated as drug candidates for cancer and fibrotic diseases, in which the Wnt pathways are aberrantly activated. Tankyrase is also reported to degrade the adaptor protein SH3BP2 (SH3 domain-binding protein 2). We have previously shown that SH3BP2 gain-of-function mutation enhances receptor activator of nuclear factor- κ B ligand (RANKL)-induced osteoclastogenesis in murine bone marrow-derived macrophages (BMMs). Although the interaction between tankyrase and SH3BP2 has been reported, it is not clear whether and how the inhibition of tankyrase affects bone cells and bone mass. Here, we have demonstrated that tankyrase inhibitors (IWR-1, XAV939, and G007-LK) enhanced RANKL-induced osteoclast formation and function in murine BMMs and human peripheral blood mononuclear cells through the accumulation of SH3BP2, subsequent phosphorylation of SYK, and nuclear translocation of NFATc1. Tankyrase inhibitors also enhanced osteoblast differentiation and maturation, represented by increased expression of osteoblast-associated genes accompanied by the accumulation of SH3BP2 protein and enhanced nuclear translocation of ABL, TAZ, and Runx2 in primary osteoblasts. Most importantly, pharmacological inhibition of tankyrase in mice significantly decreased tibia and lumbar vertebrae bone volumes in association with increased numbers of osteoclasts. Our findings uncover the role of tankyrase inhibition in bone cells and highlight the potential adverse effects of the inhibitor on bone.

© 2017 Elsevier Inc. All rights reserved.

1. Introduction

Tankyrase (tankyrase 1 and 2) is a member of the poly(ADP-ribose) polymerase (PARP) family [1]. Tankyrase, also known as PARP5, interacts with target proteins and catalyzes poly(ADP-ribosyl)ation, leading to polyubiquitination and degradation of the target proteins [1]. One of the target proteins is AXIN, a negative regulator of the canonical Wnt/ β -catenin pathway [2]. Tankyrase induces the degradation of AXIN and subsequently upregulates Wnt/ β -catenin signaling [2]. Thus, tankyrase inhibitors operate as Wnt/ β -catenin inhibitors through the accumulation of AXIN [2]. Tankyrase inhibitors are attracting attention as promising therapeutic options for various cancers and fibrotic

diseases, in which increased activation of Wnt/ β -catenin pathway contributes to the pathogenesis [3–6]. Some tankyrase inhibitors are currently in preclinical testing [7,8].

Tankyrase is reported to mediate the degradation of SH3-domain binding protein 2 (SH3BP2) [9]. SH3BP2 is an adaptor protein predominantly expressed in immune cells, including macrophages/osteoclasts, as well as in osteoblasts [10,11]. SH3BP2 regulates intracellular signaling pathways such as protein tyrosine kinases ABL1 and SYK [12–14]. We have previously demonstrated that the overexpression of wild-type SH3BP2 protein in macrophages promotes receptor activator of nuclear factor- κ B ligand (RANKL)-induced osteoclastogenesis [12,15]. SH3BP2 gain-of-function mutant mice exhibit systemic osteopenia owing to aberrantly increased osteoclast formation and function in response to RANKL [12,15]. In contrast, SH3BP2 deficiency impairs osteoclast differentiation and function [11,16], which illustrates the essential role of SH3BP2 in osteoclastogenesis. Levaot et al. demonstrated that tankyrase interacts with SH3BP2 and treatment with a tankyrase inhibitor increases osteoclast formation in cultured bone marrow-derived macrophages (BMMs) [9]. Therefore, while tankyrase inhibitor has the

Abbreviations: PARP, poly(ADP-ribose) polymerase; SH3BP2, SH3 domain-binding protein 2; BMMs, bone marrow-derived macrophages; WT, wild-type; MNCs, multinucleated cells; CBP, CREB-binding protein; OIM, osteogenic induction medium.

* Corresponding author at: Department of Rheumatology, Kawasaki Medical School, 577 Matsushima, Kurashiki, Okayama 701-0192, Japan.

E-mail address: mukai@med.kawasaki-m.ac.jp (T. Mukai).

potential to affect bone volume, no studies exploring the influence of pharmacological tankyrase inhibition *in vivo* have been conducted.

It is highly likely that tankyrase is also involved in osteoblast differentiation. Osteoblasts express AXIN and SH3BP2 and their intracellular stability is regulated by tankyrase. AXIN negatively regulates osteoblastogenesis through suppressing Wnt/ β -catenin signaling [17,18]. Interestingly, it has been reported that SH3BP2-deficient mice exhibit osteoporosis due to defective osteoblastogenesis [11,19]. Thus, SH3BP2 may positively regulate osteoblastogenesis. It is therefore essential to investigate whether tankyrase or tankyrase inhibition affects osteoblast differentiation and maturation.

In the present study, we investigated the *in vitro* effects of tankyrase inhibitors on osteoclasts and osteoblasts. We also set out to determine whether pharmacological inhibition of tankyrase could affect bone mass in mice.

2. Materials and methods

2.1. Mice

Wild-type (WT) C57BL/6 J male mice were purchased from CLEA Japan Inc. (Osaka, Japan). All mice were housed in groups of 3–5 per cage, and maintained at 22 °C under a 12:12 h light/dark cycle with free access to water and standard laboratory food (MF diet, Oriental Yeast Co., Tokyo, Japan). All animal experiments were approved by the Animal Research Committee of Kawasaki Medical School (Nos. 14-094, 14-102, and 15-088). All experimental procedures were conducted in accordance with institutional and NIH guidelines for the humane use of animals.

2.2. Reagents and antibodies

Recombinant murine and human M-CSF and RANKL proteins were purchased from Peprotech (Rocky Hill, NJ, USA). IWR-1-endo (IWR-1) was purchased from Santa Cruz Biotechnology (Santa Cruz, CA, USA). G007-LK, XAV939, and ICG-001 were purchased from Selleck Chemicals (Houston, TX, USA). FK506 was obtained from Sigma-Aldrich (St. Louis, MO, USA). Anti-SH3BP2 antibody (H00006452-M01) was obtained from Abcam (Cambridge, MA, USA). Anti-ACTIN antibody (A2066) was obtained from Sigma-Aldrich. Anti-Phospho-SYK (Tyr352) antibody (2701), anti-total SYK antibody (13198), anti-NUP98 antibody (2598), anti-GAPDH antibody (2118), anti-c-FOS antibody (2250), anti-AXIN1 antibody (2074), anti- β -catenin antibody (8480), anti-RUNX2 antibody (8486), HRP-conjugated anti-rabbit IgG antibody (7074), and HRP-conjugated anti-mouse IgG antibody (7076) were obtained from Cell Signaling Technology (Danvers, MA, USA). Anti-NFATc1 antibody (sc-7294), anti-NF- κ B p50 antibody (sc-1190), anti-ABL antibody (sc-56,887), and HRP-conjugated anti-goat IgG antibody (sc-2354) were obtained from Santa Cruz Biotechnology.

2.3. Osteoclast differentiation assay

Primary mouse bone marrow cells were isolated from the long bones of 6- to 10-week-old WT mice as previously described [12,20]. Bone marrow cells were cultured on Petri dishes for 2–4 h at 37 °C in 5% CO₂. To minimize the contamination of stromal cells, only non-adherent cells were collected and used for the following bone marrow cell cultures. Non-adherent bone marrow cells were seeded on 48-well plates at a density of 5.0×10^4 cells/well and incubated for 2 days in α -MEM supplemented with 10% FBS containing M-CSF (25 ng/mL) at 37 °C in 5% CO₂. After preculture for 2 days, BMMs were stimulated with M-CSF (25 ng/mL) and RANKL at the indicated concentrations for an additional 3 days in the presence of the tankyrase inhibitors (IWR-1, XAV939, and G007-LK). BMMs were seeded at a density of 0.5×10^5 cells/well on 48-well plates. The formation of tartrate-resistant acid phosphatase (TRAP)-positive multinucleated cells (TRAP+ MNCs)

was visualized by TRAP staining (Sigma-Aldrich). TRAP+ MNCs with three or more nuclei were counted as osteoclasts. Murine pre-osteoclastic RAW264.7 cells were obtained from ATCC (Manassas, VA, USA). To investigate osteoclast differentiation, RAW264.7 cells were plated at a density of 4.0×10^3 cells/well with RANKL (50 ng/mL) in the presence of tankyrase inhibitors. The formation of TRAP+ MNCs was quantified after 4 days of treatment with RANKL treatment. TRAP activity in culture supernatant was determined as described previously [12].

To compare against other tankyrase inhibitors, we used a β -catenin/CBP inhibitor, ICG001, which belongs to another class of Wnt inhibitors. ICG001 is a small molecule that specifically inhibits T-cell factor/ β -catenin transcription in a CREB-binding protein (CBP)-dependent fashion. ICG001 selectively blocks the β -catenin/CBP interaction without interfering with the β -catenin/p300 interaction [21].

2.4. Resorption assay

To quantify the mineral resorbing activity of osteoclasts, a resorption assay was performed on calcium phosphate-coated plates [12,16]. Bone marrow cells were plated at 2.0×10^4 cells/well on Osteo Assay Surface 96 Well Multiple Well Plates (Corning Inc., Corning, NY, USA) and cultured with M-CSF (25 ng/mL) and RANKL (50 ng/mL) in the presence of tankyrase inhibitors (IWR-1, G007-LK) or β -catenin/CBP inhibitor (ICG001) for 10 days. Resorption areas were visualized by von Kossa staining. Images were acquired via a BZX-700 microscope (Keyence, Osaka, Japan), and the resorption area was quantified using ImageJ software (NIH, Bethesda, MD). The resorption area was calculated as a percentage of the total area of the calcium phosphate-coated well.

2.5. Real-time quantitative PCR (qPCR)

Total RNA was extracted using RNAiso Plus (Takara Bio, Shiga, Japan) and solubilized in RNase-free water as previously described [12,20]. cDNA was synthesized using Prime Script RT reagent Kit (Takara Bio). qPCR reactions were performed using SYBR Green PCR Master Mix (Takara Bio) with StepOne Plus System (Thermo Fisher Scientific, Waltham, MA, USA). Gene expression levels relative to *Hprt* were calculated by $\Delta\Delta$ Ct method and normalized to baseline controls as indicated in each experiment. The qPCR primers used in this study are listed in Supplemental Table 1. All qPCR reactions yielded products with single peak dissociation curves.

2.6. Western blot

For western blot analysis, cells were washed with ice-cold PBS and lysed with RIPA lysis buffer (Sigma-Aldrich) with protease and phosphatase inhibitor cocktails (Sigma-Aldrich) [12,16]. For nuclear and cytoplasmic fractionation, cells were lysed on ice in cytoplasmic lysis buffer (10 mM HEPES (pH 7.9), 1.5 mM MgCl₂, 10 mM KCl, 0.5 mM DTT, 0.05% Igepal), and nuclei were sedimented by centrifugation and lysed in nuclear lysis buffer (2% SDS, 2 M urea, 8% sucrose, 20 mM sodium β -glycerophosphate, 1 mM NaF, and 5 mM Na₂VO₄). Protein concentrations were determined by BCA Protein Assay Kit (Thermo Fisher Scientific). Protein samples were resolved by SDS-PAGE and transferred to nitrocellulose membranes. After blocking with 5% skim milk or 5% BSA in TBST buffer, membranes were incubated with primary antibodies, followed by incubation with appropriate HRP-conjugated species-specific secondary antibodies. Bands were detected using SuperSignal West Dura or Femto chemiluminescent substrate (Thermo Fisher Scientific) and visualized by ImageQuant LAS-4000 (GE Healthcare, Little Chalfont, UK). ACTIN, GAPDH, and nuclear pore complex proteins Nup98-Nup96 (NUP98) were used as loading controls to normalize the amount of protein in the indicated fractions.

2.7. Human peripheral blood mononuclear cells (PBMCs) experiments

Whole blood was obtained from a healthy donor under a protocol approved by the Research Ethics Committee of Kawasaki Medical School (No. 2563). The donor provided prior informed consent. PBMCs were isolated from whole blood by density gradient separation using Lymphoprep (Axis-Shield, Oslo, Norway) [22]. PBMCs were cultured on 100-mm dishes with human M-CSF (20 ng/mL) at 37 °C in a 5% CO₂ atmosphere to generate osteoclast precursor cells for 9 days. Cells (2×10^5 cells/mL) were then seeded into the indicated plates and stimulated with M-CSF (20 ng/mL) and RANKL (25 ng/mL) in the presence of IWR-1 (1 μM), G007-LK (0.1 μM), ICG001 (1 μM), or olaparib (0.1 μM, a PARP1 inhibitor). To determine osteoclast differentiation and function, TRAP staining, fluorescent staining, and a resorption assay were performed at specific time points.

2.8. Immunofluorescent staining

RAW264.7 cells (4.0×10^3 /well) were plated onto 8-well chamber slides (BD Falcon, Franklin Lakes, NJ, USA) and stimulated with RANKL (50 ng/mL) for an additional 4 days in the presence of IWR-1 or XAV939. The cells were fixed in 4% PFA, permeabilized using 0.2% Triton X-100, blocked in 2% normal goat serum/2.5% BSA/PBS, and incubated with anti-NFATc1 antibody at 4 °C overnight [12,20]. NFATc1 was detected by Alexa Fluor-555-conjugated goat anti-mouse IgG antibody (Thermo Fisher Scientific), and ACTIN and the nuclei were co-stained with Alexa Fluor-488-conjugated phalloidin (Thermo Fisher Scientific) and DAPI (Santa Cruz Biotechnology), respectively. Fluorescent images of the cells were acquired with a BZX-700 microscope. Primary BMMs and PBMCs were also stained with Alexa Fluor-488-conjugated phalloidin and DAPI.

2.9. Osteoblast differentiation assay

Primary osteoblasts were prepared from the calvaria of 3–6-day-old neonatal WT mice by the sequential enzymatic digestion method [23, 24]. In brief, the calvaria were gently incubated with 0.2% collagenase and 0.1% trypsin in α-MEM at 37 °C for 15 min, and cells were collected in supernatants. Incubation was repeated six consecutive times. Cells obtained during the last five digestion processes were harvested collectively in α-MEM containing 10% FBS, followed by centrifugation at $430 \times g$ for 5 min. The pellets were suspended in α-MEM containing 10% FBS. Cells were plated at a density of 4.0×10^4 cells/mL in appropriate dishes and cultured for indicated periods at 37 °C under 5% CO₂ with a change in media every 3 days. Throughout the experiments, osteogenic induction medium (OIM) consisting of α-MEM, 10% FBS, 50 μg/mL ascorbic acid, and 2 mM sodium β-glycerophosphate were used to promote osteoblastic differentiation. To perform alizarin red staining, cells were fixed with 95% ethanol, washed twice with water, and incubated with 2% alizarin red staining solution (pH 4.2) for 10 min at room temperature, followed by five subsequent washes with water. To quantify mineralization of the matrix, the area of the nodules was analyzed using ImageJ software ($n = 3$ wells/group) [23].

2.10. In vivo tankyrase inhibitor (G007-LK) administration

Seven-week-old WT male mice were fed on a diet containing 400 μg/day of G007-LK for 4 weeks. Mice were housed in groups of two per plastic cage. Food intake per cage was monitored daily and body weights were recorded weekly. After 4 weeks, right hind limbs, lumbar vertebrae (L6), and serum samples were obtained from the mice following euthanasia under sevoflurane-induced anesthesia. We used these samples for the analysis of micro computed tomography (micro-CT), histology, and ELISA as described below.

2.11. Micro-CT analysis

Bone samples were fixed in 4% PFA in PBS for 2 days, and PFA-fixed hind limbs and lumbar vertebrae were immersed in 70% ethanol. Three-dimensional trabecular microarchitectures of the right tibias and vertebrae were evaluated using a micro-CT system (Ele Scan mini; Nittetsu Elex, Tokyo, Japan) with an X-ray energy of 45 kVp (145 μA) [12,25]. The voxel resolution of the tibia is 10 μm, and that of the vertebra is 15 μm. The trabecular and cortical bone properties of tibias and lumbar vertebrae were analyzed using 3D image analysis software (TRI/3D-BON; Ratoc System Engineering, Tokyo, Japan). The region of trabecular bone analyzed in tibias comprised 100 slices of secondary spongiosa immediately adjacent to the primary spongiosa (starting 0.5 mm from the distal border of the growth plate); that of the vertebrae comprised the entire vertebral body area (approximately 140 slices); and that of cortical bone comprised 50 slices of the midshaft (1 mm proximal to the tibiofibular junction) of the tibia. All micro-CT parameters are described according to international guidelines [26].

2.12. Histological analysis

Bone samples were fixed in 4% PFA in PBS for 2 days, decalcified for 4 weeks in 10% EDTA (pH 7.2) at 4 °C, and then embedded in paraffin. Sections (3 μm) were stained with hematoxylin and eosin (H&E). TRAP staining was performed to visualize TRAP-positive cells, and the sections were counterstained with methyl green. Histological measurements were performed in a blinded manner using ImageJ software. The number of osteoclasts per bone surface (N·Oc/BS) and osteoclast surface per bone surface (Oc.S/BS) were determined. The terminology and units are described according to international recommendation [27].

2.13. ELISA assay

Mouse TRAP isoform 5b (TRAP5b), amino-terminal propeptide of type I procollagen (PINP), and osteocalcin (OCN) concentrations in serum were measured with mouse TRAP™ Assay (Immunodiagnostic Systems, Tyne, UK), mouse PINP ELISA kit (MyBioSource, San Diego, CA, USA), and mouse osteocalcin EIA kit (Biomedical Technologies Inc., Stoughton, MA, USA), respectively. All assays were batched and run simultaneously with a single kit according to the manufacturers' protocols.

2.14. Statistical analysis

All values are given as means ± SD. Statistical analysis was performed by the two-tailed unpaired Student's *t*-test to compare two groups and one-way ANOVA (Tukey post-hoc test) to compare three or more groups using GraphPad Prism 5 (GraphPad Software, San Diego, CA, USA). *P* values < 0.05 were considered statistically significant.

3. Results

3.1. Tankyrase inhibitors enhanced RANKL-induced osteoclast differentiation and function in BMMs

To thoroughly examine the effect of tankyrase inhibitors on osteoclastogenesis, we used three small molecules (IWR-1, G007-LK, and XAV939), all of which specifically inhibit tankyrase activity [28]. IWR-1 and XAV939 are widely used in pharmacological experiments, and G007-LK is a newly developed inhibitor with higher bioavailability [3]. We found that treatment with the three tankyrase inhibitors in BMMs culture increased RANKL-induced TRAP+ MNCs formation in a dose-dependent manner (Fig. 1A, B, Supp. Fig. 1A). TRAP activity in culture medium was also significantly increased in tankyrase inhibitor-treated BMM cultures (Supp. Fig. 1B), and IWR-1 promoted actin ring formation

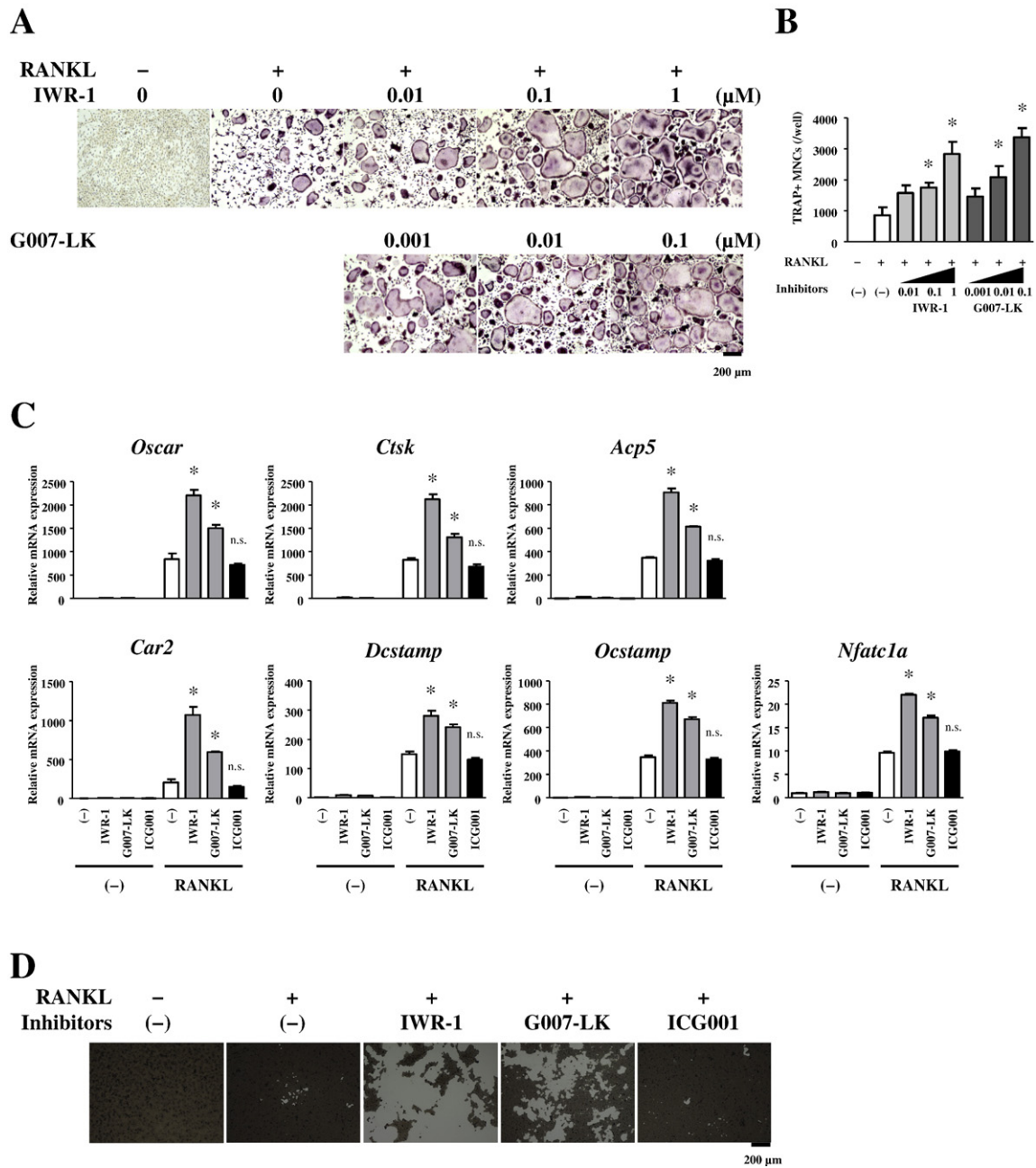


Fig. 1. Tankyrase inhibitors enhanced receptor activator of nuclear factor- κ B ligand (RANKL)-induced osteoclast differentiation and function. Bone marrow cells were isolated from wild-type (WT) mice. Non-adherent bone marrow cells were seeded at a density of 5.0×10^4 per well on 48-well plates. After 2-day preculture with M-CSF (25 ng/mL), bone marrow-derived macrophages (BMMs) were stimulated with RANKL in the presence of tankyrase inhibitors at indicated concentrations for 72 h. (A) Tartrate-resistant acid phosphatase (TRAP) staining images of BMMs stimulated with RANKL in the presence of tankyrase inhibitors at indicated concentrations for 72 h. (B) Quantitation of TRAP-positive multinucleated cells (TRAP + MNCs) per well. (C) qPCR analysis of osteoclast-associated gene expression. Bone marrow cells were isolated from WT mice. After preculture for 2 days with M-CSF (25 ng/mL), BMMs were stimulated with RANKL (10 ng/mL) in the presence of IWR-1 (2 μM), G007-LK (0.1 μM), or ICG001 (2 μM) for 48 h. Gene expression levels relative to *Hprt* were calculated and normalized to the level of expression of non-treated control cells at 48 h. (D) Resorption assays: BMMs were cultured with RANKL (50 ng/mL) in the presence of IWR-1 (2 μM), G007-LK (0.1 μM), or ICG001 (2 μM) on calcium phosphate-coated plates for 10 days. After removal of the cells, resorption areas were visualized by von Kossa staining. Data are presented as means \pm SD. * $P < 0.05$ compared to RANKL-treated cells without an inhibitor. n.s. = not significant.

in response to RANKL (Supp. Fig. 1C). The tankyrase inhibitors alone did not induce the formation of TRAP + MNCs without RANKL stimulation (data not shown).

We measured the mRNA expression levels of genes associated with osteoclastogenesis, such as osteoclast-associated receptor (*Oscar*), cathepsin K (*Ctsk*), acid phosphatase 5 (*Acp5*), carbonic anhydrase II (*Car2*), dendritic cell-specific transmembrane protein (*Dcstamp*), osteoclast stimulatory transmembrane protein (*Ocstamp*), and nuclear factor of activated T-cells cytoplasmic 1 (NFATc1) isoform A (*Nfatc1a*) [12,16]. qPCR analysis revealed that the tankyrase inhibitors significantly

increased the expression of these osteoclast-associated genes in BMMs 48 h after RANKL stimulation (Fig. 1C).

We next examined osteoclast function by mineral resorption assay. The tankyrase inhibitors dramatically enhanced the area of calcium phosphate resorption (Fig. 1D). In murine preosteoclastic RAW264.7 cell cultures, as well as in primary BMMs, tankyrase inhibitors increased TRAP + MNCs formation, actin ring formation, and the expression of osteoclast-associated genes (Supp. Fig. 2A–D). In accordance with previous findings [9], these results demonstrated that tankyrase inhibitors enhanced osteoclast formation and function.

Tankyrase inhibitors are reported to have a suppressive effect on the Wnt/ β -catenin signaling pathway [3]. We also compared the effects on osteoclastogenesis between tankyrase inhibitors and ICG001, a β -catenin/CBP inhibitor [21]. We found that ICG001 did not promote the formation of RANKL-induced TRAP+ MNCs (data not shown), the expression of osteoclast-associated genes (Fig. 1C), or resorption activity (Fig. 1D). These results suggest that the osteoclast-inducing effect of tankyrase inhibitors is unlikely to be mediated by the inhibition of Wnt/ β -catenin signaling.

3.2. Tankyrase inhibitors stabilized SH3BP2 and subsequently activated SYK and NFATc1 in RANKL-stimulated BMMs

Tankyrase is reported to degrade SH3BP2 protein [9]. In the present study, we found that both IWR-1 and G007-LK elevated the levels of SH3BP2 protein (Fig. 2A) while the mRNA levels were unchanged (Fig. 2B), confirming the post-transcriptional regulation of SH3BP2 protein by tankyrase inhibitors. We further investigated intracellular signaling. SYK is an SH3BP2-binding partner, and phosphorylated SYK controls downstream signaling events that lead to the activation of NFATc1, a master transcription factor for osteoclastogenesis [12,15,29]. We found that the phosphorylation of SYK increased in the presence of IWR-1 (Fig. 2C). Immunoblot analysis revealed that RANKL induced nuclear localization of NFATc1, and IWR-1 dramatically augmented the expression of NFATc1 compared to that of non-treated BMMs at 48–96 h (Fig. 2D). Moreover, immunofluorescent staining revealed that tankyrase inhibitors also increased NFATc1 nuclear expression in RAW264.7 cells (Supp. Fig. 3). To confirm whether NFATc1 functions downstream of tankyrase inhibition, IWR-1-treated BMMs were treated with a calcineurin inhibitor FK506 in the presence of RANKL. FK506

diminished the osteoclast-promoting effect of the tankyrase inhibitor in a dose-dependent manner (Supp. Fig. 1D). These results indicate that NFATc1 is a crucial downstream target of tankyrase inhibitors in osteoclasts.

Nuclear translocation of NF- κ B and c-FOS has been shown to precede the robust induction of NFATc1 [12,29]. Therefore, we examined the protein levels in the nuclei to determine whether tankyrase inhibitors enhance NF- κ B and c-FOS activation prior to the induction of NFATc1. RANKL induced nuclear localization of NF- κ B (p50) and c-FOS at 48 h, but IWR-1 treatment did not affect the expression levels of these transcription factors (Fig. 2E). Collectively, these results indicate that tankyrase inhibitors promote osteoclast formation via increased phosphorylation of SYK and subsequent nuclear translocation of NFATc1 without affecting NF- κ B and c-FOS pathways.

3.3. Tankyrase inhibitors enhanced osteoclast differentiation and function in human PBMCs

Some functional differences have been reported between human and mouse tankyrases [30]. We therefore examined whether tankyrase inhibitors could promote osteoclastogenesis in human macrophages. We found that tankyrase inhibitors increased the formation of TRAP+ MNCs, the formation of the actin ring, and mineral resorbing activity (Fig. 3A, B), indicating that tankyrase inhibition enhances osteoclast formation and function in human PBMCs as well as mouse BMMs.

To examine whether the enhancement of osteoclastogenesis is mediated specifically by tankyrase (also known as PARP5), we tested the effect of a PARP1 inhibitor, olaparib, on osteoclastogenesis. Olaparib is clinically approved anti-cancer drug for ovarian cancer and breast cancer [31,32]. In contrast to the apparent effect of tankyrase inhibitors,

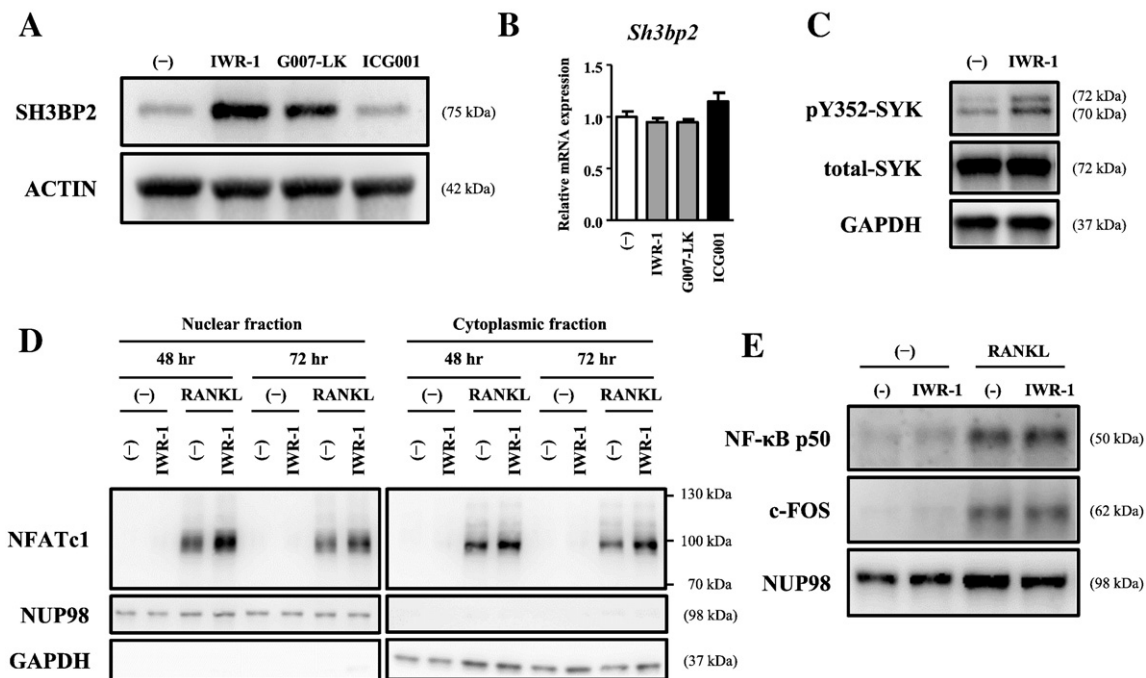


Fig. 2. Tankyrase inhibitors augmented the nuclear translocation of NFATc1 via the accumulation of SH3BP2. Bone marrow cells were isolated from WT mice. After preculture for 2 days with M-CSF (25 ng/mL), cells were stimulated with RANKL (50 ng/mL) in the presence of IWR-1, G007-LK, or ICG001. Protein samples were collected at the indicated time points. (A) Western blot analysis of SH3BP2 in WT BMMs after culture for 2 days in the presence of IWR-1 (2 μ M), G007-LK (0.1 μ M), or ICG001 (2 μ M). (B) qPCR analysis of *Sh3bp2* in WT BMMs. BMMs were cultured in the presence of IWR-1 (2 μ M), G007-LK (0.1 μ M), or ICG001 (2 μ M) for 48 h. Gene expression levels relative to *Hprt* were calculated and normalized to the level of expression of non-treated control cells at 48 h. (C) Western blot analysis of the phosphorylation of SYK stimulated with RANKL (50 ng/mL) in the presence of IWR-1 (2 μ M) at 48 h. (D) Western blot analysis of NFATc1. NFATc1 expression levels in nuclear and cytoplasmic fractions were determined at the indicated time points. (E) Western blot analysis of NF- κ B and c-FOS in nuclear fractions at 48 h.

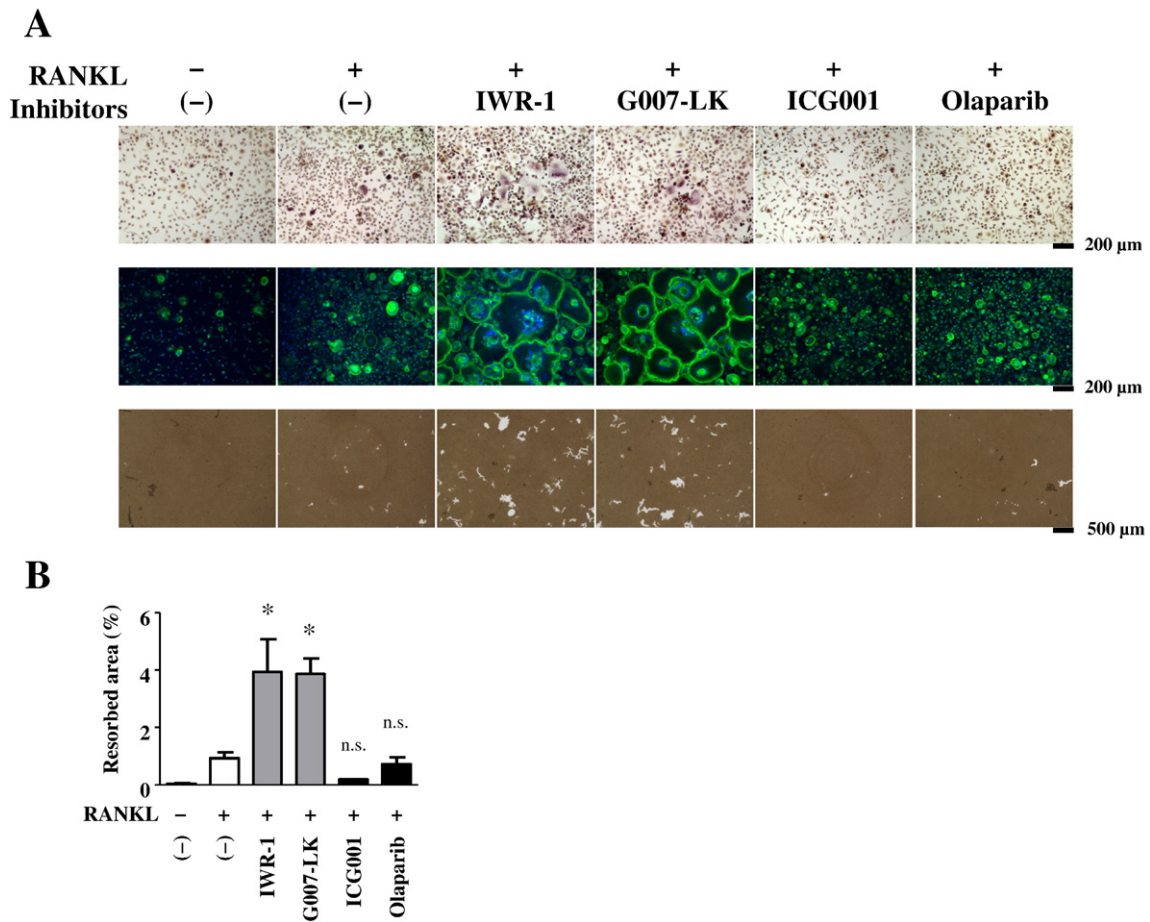


Fig. 3. Tankyrase inhibitors promoted osteoclast differentiation and function in human peripheral blood mononuclear cells (PBMCs). Human PBMCs were isolated in a blood sample from a healthy individual. After preculture for 9 days with M-CSF (20 ng/mL), cells were stimulated with RANKL (25 ng/mL) in the presence of IWR-1 (1 μ M), G007-LK (0.1 μ M), ICG001 (1 μ M), or olaparib (0.1 μ M). (A) (Top) TRAP staining images of PBMCs stimulated with RANKL in the presence of inhibitors at 8 days. (Middle) Fluorescent staining of RANKL-stimulated PBMCs. Cells were fixed at 8 days. ACTIN and nuclei were visualized with Alexa Fluor-488-conjugated phalloidin (green) and DAPI (blue), respectively. (Bottom) Resorption assay. The resorbed area was visualized by von Kossa staining after RANKL treatment for 12 days. (B) Resorbed areas (%) on calcium phosphate-coated plates were quantified ($n = 3$ per group). Data are presented as means \pm SD. * $P < 0.05$ compared to RANKL-treated cells without an inhibitor. n.s. = not significant.

olaparib did not affect osteoclastogenesis in human PBMCs (Fig. 3A, B), suggesting that the promotion of osteoclastogenesis by tankyrase inhibitors is not mediated by non-specific PARsylation.

3.4. Tankyrase inhibitors enhanced osteoblast differentiation despite their Wnt inhibitory effect

We subsequently examined whether tankyrase inhibitors could affect osteoblast differentiation and maturation. Murine primary calvaria cells were cultured with tankyrase inhibitors (IWR-1, G007-LK) or β -catenin/CBP inhibitor (ICG001) in osteogenic induction medium containing ascorbic acid and β -glycerophosphate. We first analyzed the expression of osteoblast differentiation marker genes—runt-related transcription factor-2 (*Runx2*), osterix (*Osx*), alkaline phosphatase (*Alp*), osteocalcin (*Ocn*), and bone sialoprotein (*Bsp*)—by qPCR analysis. We found that the tankyrase inhibitors had significantly increased the expression of *Runx2*, *Osx*, and *Alp* mRNA on day 14 (Fig. 4A). Moreover, treatment with tankyrase inhibitors had dramatically increased *Ocn* expression by 5- to 8-fold and *Bsp* expression by 3- to 5-fold on day 14 (Fig. 4A). Alizarin red staining showed that tankyrase inhibitors significantly increased mineralization (Fig. 4B, C). These findings were in contrast with those of ICG-001-treated cells, which significantly suppressed the expression of osteoblast marker genes and mineral deposition (Fig. 4A-C). These results suggest that tankyrase inhibitors promote osteoblast differentiation and maturation, even though the inhibitors have a suppressive effect on Wnt/ β -catenin signaling [3].

3.5. Tankyrase inhibitors enhanced nuclear translocation of ABL and RUNX2 in primary osteoblasts

We evaluated intracellular signaling during osteoblast differentiation using murine primary calvaria cells. Immunoblot analysis revealed that tankyrase inhibitors IWR-1 and G007-LK increased the expression of both AXIN and SH3BP2 proteins, whereas ICG001 had no effect on expression (Fig. 5A). It is worth noting that tankyrase inhibitors suppressed the nuclear expression of β -catenin (Fig. 5B), reflecting their Wnt inhibitory effect.

ABL, a tyrosine kinase, binds to and is activated by SH3BP2 [33]. It was recently reported that activated ABL assembles the transcriptional factor complex of RUNX2 and transcriptional coactivator with the PDZ-binding motif (TAZ) required for the differentiation of osteoblasts [19]. We found that IWR-1 and G007-LK enhanced the nuclear localization of ABL, TAZ, and RUNX2 (Fig. 5C, D).

3.6. Tankyrase inhibitor induced bone loss in wild-type mice in vivo

To investigate whether the administration of a tankyrase inhibitor affects bone mass in mice, seven-week-old WT male mice were fed on a diet containing G007-LK for 4 weeks, and then their tibias and lumbar vertebrae were analyzed by micro-CT and histology. We tested G007-LK in this study because it has greater in vivo stability and bioavailability than other tankyrase inhibitors such as IWR-1 or XAV939 [3]. Body

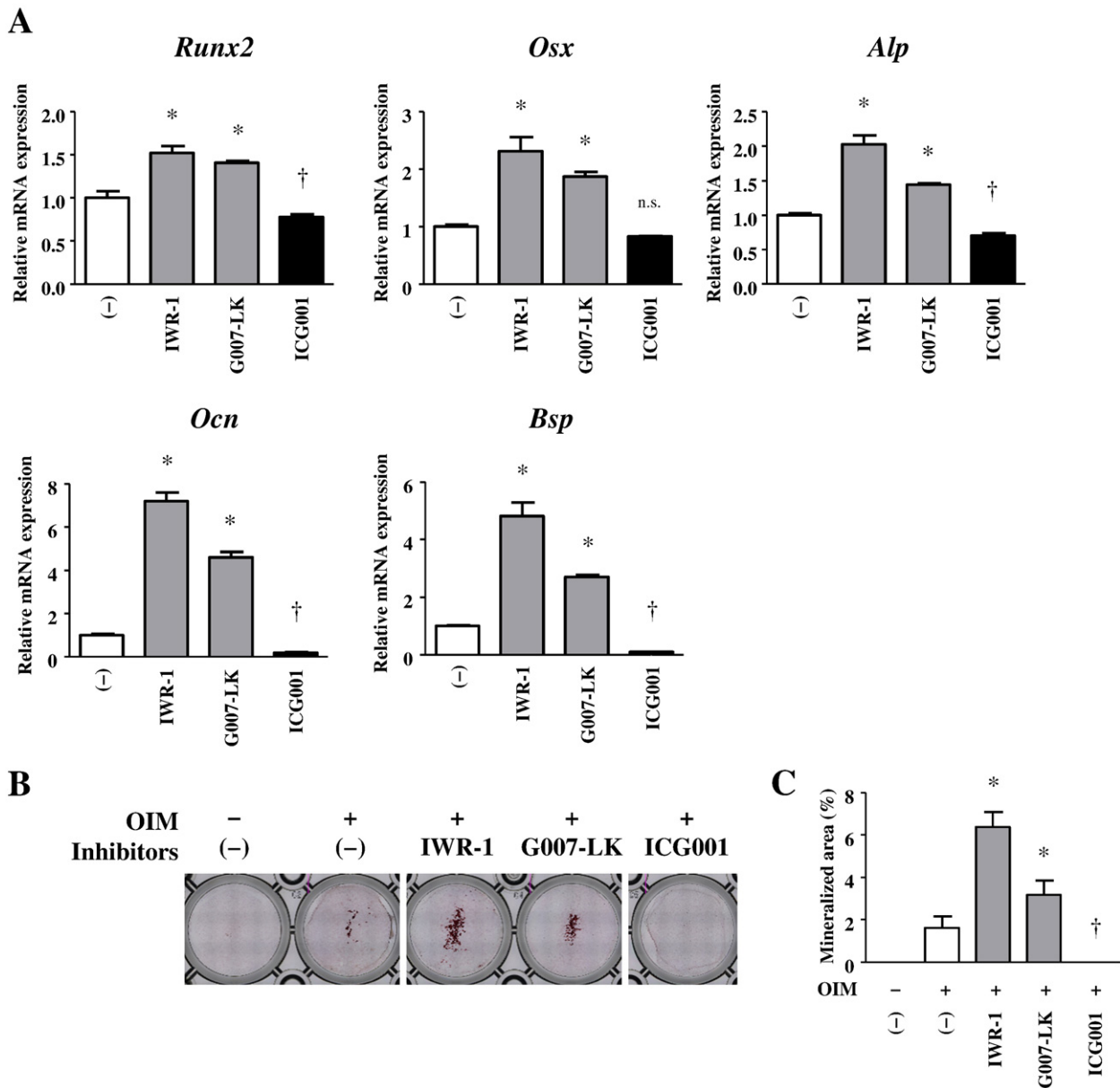


Fig. 4. Tankyrase inhibitors enhanced osteoblast differentiation and mineralization. Primary calvaria cells isolated from WT pups were cultured in the presence of IWR-1 (3 μ M), G007-LK (0.3 μ M), or ICG001 (3 μ M) in osteogenic induction medium (OIM). (A) qPCR analysis of osteoblast-associated gene expression. Primary calvaria cells were cultured in the presence of IWR-1, G007-LK, or ICG001 for 14 days. Gene expression levels relative to *Hprt* were calculated and normalized to the expression level of the cells cultured in OIM without inhibitors. (B) Alizarin red staining images at day 24. (C) Quantitation of mineral nodule formation by alizarin red staining images at 24 days. Data are presented as means \pm SD. * indicates a significant increase ($P < 0.05$) compared to RANKL-treated cells without an inhibitor. † indicates a significant decrease ($P < 0.05$). n.s. = not significant.

weights and food intake were not affected by G007-LK administration (Supp. Fig. 4A, B). No behavioral abnormalities were detected during the observation period. Micro-CT analysis revealed that the trabecular bone volume (BV/TV) of proximal tibiae was significantly decreased by approximately 30% in G007-LK-treated mice compared with control mice (Fig. 6A, B). Cortical bone thickness (Ct.Th) at the midshaft of the tibiae was also significantly decreased in G007-LK-treated mice (Fig. 6C, D). The BV/TV of lumbar vertebrae was significantly decreased by approximately 22% (Fig. 6E, F). A reduction in bone volume was also observed in histological sections of tibiae and vertebrae (Fig. 7A).

The analysis of TRAP stained tibiae revealed that osteoclast numbers and surface areas were significantly increased in G007-LK-treated mice compared to control mice (Fig. 7B, C). Accordingly, the serum TRAP5b level tended to be higher in G007-LK-treated mice compared to control mice (Fig. 7D). There were no significant differences in the serum levels

of PINP and OCN between G007-LK-treated mice and control mice (Fig. 7E, F).

4. Discussion

Tankyrase inhibitors have been investigated as promising drug candidates for cancer and fibrotic diseases, during which the Wnt pathways are aberrantly activated [3–7]. However, tankyrase inhibitors might have adverse effects on bone tissue. In this study, we investigated the effects of the pharmacological inhibition of tankyrase on bone metabolism in vitro and in vivo. We observed that tankyrase inhibitors enhanced osteoclast differentiation and function through the accumulation of SH3BP2 in murine macrophages and human PBMCs. In murine primary osteoblasts cultures, tankyrase inhibitors promoted osteoblast differentiation and maturation, despite the suppression of Wnt/ β -catenin signaling. Most importantly, systemic administration of a tankyrase

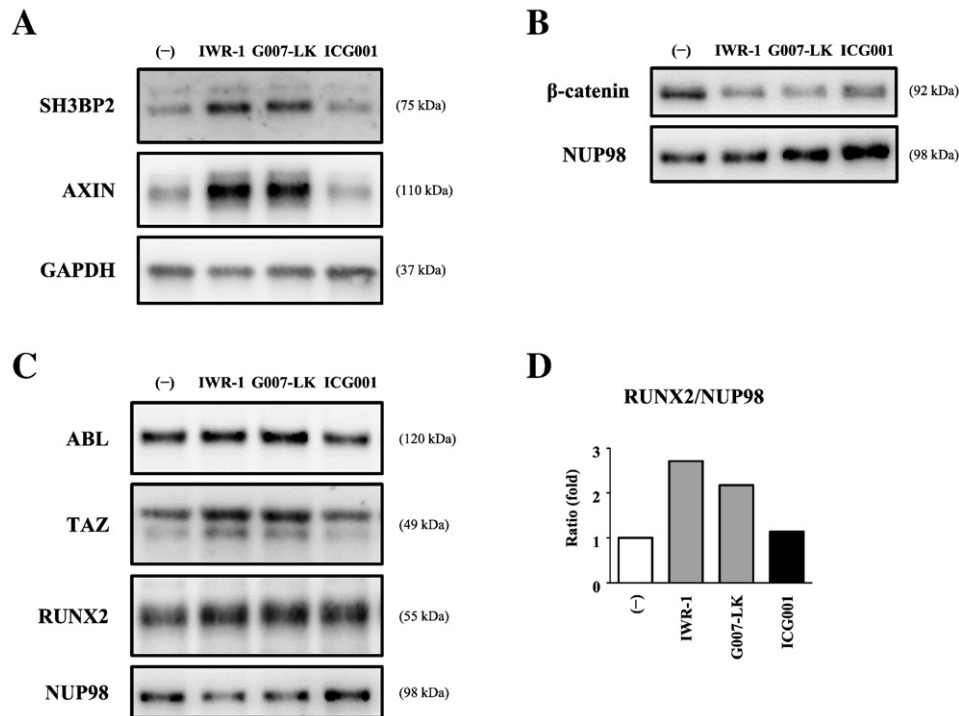


Fig. 5. Osteoblast-promoting effect of tankyrase inhibitors. Primary calvaria cells isolated from WT pups were cultured in the presence of IWR-1 (3 μ M), G007-LK (0.3 μ M), or ICG001 (3 μ M) in OIM. Nuclear and cytoplasmic protein samples were collected at indicated time points and subjected to Western blot analysis of the indicated proteins. (A) Western blot analysis of SH3BP2 and AXIN in the cytoplasmic fraction after culture for 10 days. (B) Western blot analysis of β -catenin in the nuclear fraction after culture for 7 days. (C) Western blot analysis of ABL, TAZ, and RUNX2 in the nuclear fraction after culture for 7 days. (D) The intensities of the bands were quantified, and the ratio of RUNX2 to NUP98 was calculated and normalized to that of non-treated cells.

inhibitor resulted in bone loss with increased numbers of osteoclasts in mice.

Tankyrase (tankyrase 1 and 2) is ubiquitously expressed in various tissues [1]. Tankyrase 1 and tankyrase 2 generally have overlapping functions, shown by the development of subtle phenotypes on the deletion of either gene [9,34]. Since double knockout mice of both tankyrase 1 and 2 genes show embryonic lethality [34], Levaot et al. generated radiation chimeric mice lacking tankyrase 1 and 2 in hematopoietic cells. In these mice, tankyrase 1 was knocked down in tankyrase 2-deficient bone marrow cells by using a lentivirus harboring tankyrase 1-specific shRNA, and the infected bone marrow cells were transplanted into tankyrase 2-deficient mice. The group reported that the depletion of tankyrase 1 and 2 in hematopoietic cells results in an osteopenic phenotype associated with increased numbers of osteoclasts [9]. Our results, showing that the pharmacological inhibition of tankyrase causes significant bone loss, are consistent with the results obtained in the genetic deletion model in hematopoietic cells.

We aimed to further explore the detailed mechanisms by which tankyrase inhibition promotes osteoclastogenesis, and obtained several pieces of additional data. First, all three tankyrase inhibitors (IWR-1, XAV939, and G007-LK) enhanced RANKL-induced osteoclast formation and function in murine BMMs, RAW264.7 cells, and human PBMCs. Second, tankyrase inhibitors significantly increased the expression of osteoclast-associated genes such as *Oscar*, *Ctsk*, *Acp5*, *Car2*, *Dcstamp*, *Ocstamp*, and *Nfatc1a* in RANKL-stimulated BMMs. Third, tankyrase inhibitors increased the phosphorylation of SYK and the subsequent nuclear translocation of NFATc1 in RANKL-stimulated BMMs, without affecting NF- κ B and c-FOS pathways. Based on these results, we concluded that the inhibition of tankyrase enhances osteoclastogenesis in murine and human cells.

Tankyrase inhibitors increased the amount of SH3BP2 protein, and led to enhanced osteoclastogenesis in murine macrophages and human PBMCs. The findings recapitulate the mechanisms underlying the human genetic disease cherubism (OMIM#118400). Cherubism is an autosomal dominant craniofacial disorder characterized by excessive

maxillary and mandibular bone resorption associated with activated osteoclasts [35,36]. Cherubism is caused by mutations in the *SH3BP2* gene [37]. Tankyrase recognizes SH3BP2 protein and represses SH3BP2 protein levels through ADP-ribosylation and subsequent ubiquitination [9]. Cherubism mutant SH3BP2 protein escapes the degradation process [9,15]. Moreover, SH3BP2 gain-of-function mice, carrying the SH3BP2 cherubism mutation, exhibit systemic osteopenia owing to aberrantly increased osteoclastogenesis due to hyper-responsiveness to RANKL [12,15]. Our in vitro data and previous reports suggest that increased amounts of SH3BP2 protein via tankyrase inhibition contribute to bone loss in mice.

Tankyrase inhibitors are classified into two types: one targets the nicotinamide subsite of the tankyrase protein, which is conserved in various PARPs (e.g. XAV939), and the other targets a unique adenosine subsite that is more potent and specific to tankyrase (e.g. IWR-1 and G007-LK) [20]. XAV939 is reported to cross-react with PARP1 and PARP2 with an IC₅₀ of 0.11 μ M and 2.2 μ M, respectively, due to the high degree of conservation of the nicotinamide subsite between PARP family members [2,38]. Thus, it has been assumed that the adenosine subsite is a more desirable target for tankyrase 1/2-specific inhibition. We did not observe any detectable differences in the effects among the three tankyrase inhibitors in this study. Furthermore, a PARP1 inhibitor olaparib did not affect osteoclastogenesis in human PBMCs. We therefore concluded that the effects of tankyrase inhibitors are mediated by tankyrase (PARP5)-specific inhibition but not by non-specific PARP inhibition.

Another interesting observation made in the present study is that the pharmacological inhibition of tankyrase promotes osteoblast differentiation and mineralization in vitro. We observed that tankyrase inhibitors increased the expression of AXIN protein and suppressed the nuclear expression of β -catenin, reflecting their Wnt inhibitory effects. These findings suggest that other molecules promote osteoblastogenesis, despite the suppression of Wnt/ β -catenin signaling. This may be explained, at least in part, by the function of SH3BP2 in osteoblasts. Osteoblasts express SH3BP2, and SH3BP2-deficient mice are reported

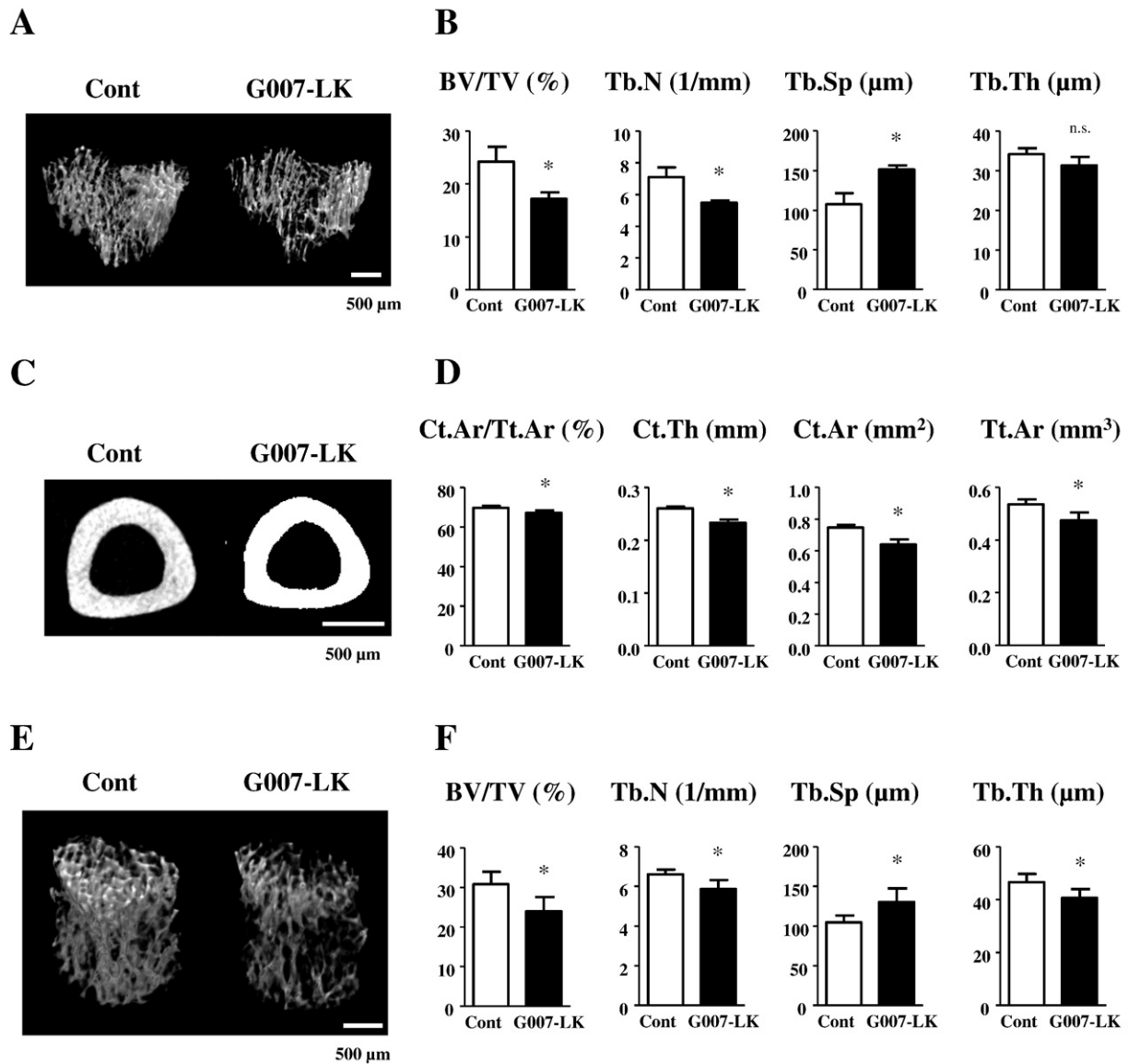


Fig. 6. Decreased bone mass in mice by pharmacological tankyrase inhibition. Seven-week-old male WT mice were fed with diets containing with G007-LK for 28 days ($n = 4$ /group). Bone samples were collected and subjected to micro-CT analysis. (A) Representative micro-CT images of the trabecular bone in the proximal tibia. (B) Bone volume per total volume (BV/TV), trabecular number (Tb.N), trabecular separation (Tb.Sp), and trabecular thickness (Tb.Th) in trabecular bone of proximal tibia. (C) Representative micro-CT images of cortical bone from the midshaft of the tibia. (D) Cortical thickness (Ct.Th), cortical area fraction (Ct.Ar/Tt.Ar), cortical bone area (Ct.Ar), and total cross-sectional area (Tt.Ar) of the midshaft of tibias (E) Representative micro-CT images of trabecular bone from lumbar vertebra. (F) Bone properties of the trabecular bone from lumbar vertebra. Data are presented as means \pm SD. * $P < 0.05$ compared to control mice. n.s. = not significant.

to exhibit osteoporosis due to defective osteoblastogenesis [11,19]. SH3BP2 activates the tyrosine kinase ABL, which is required for the differentiation of osteoblasts in association with the transcriptional coactivator TAZ [19]. We found in our study that tankyrase inhibitors increased the amount of SH3BP2 protein and the nuclear expression of ABL, TAZ, and RUNX2. This suggests that elevated levels of SH3BP2 may contribute to the activation of the ABL-TAZ complex and consequently to the acceleration of osteoblastogenesis. Other than SH3BP2-mediated pathways, tankyrase inhibitors have been reported to affect PI3K signaling and telomere shortening [39,40]. We cannot exclude the possibility that other molecules besides SH3BP2 also modulate osteoblastogenesis in tankyrase inhibitor-treated osteoblasts in vitro.

Although tankyrase inhibitors promoted osteoblast differentiation and maturation in vitro, systemic administration of the inhibitor caused significant bone loss in trabecular and cortical bones in mice. These findings may reflect a higher susceptibility of osteoclasts to tankyrase inhibitors than osteoblasts. Indeed, G007-LK promoted RANKL-induced

osteoclast formation at an even lower concentration (0.01 μ M) (Fig. 1A). On the other hand, the osteoblast-promoting effect appeared at a higher concentration (0.3 μ M) of G007-LK (Fig. 4), while a lower concentration (0.01 μ M) did not promote osteoblast differentiation or mineralization (data not shown). Another possible consideration is that the in vivo effects of tankyrase inhibitors on osteoblasts may be modulated by several indirect mechanisms via other cells. In our study, serum PINP and OCN levels were not elevated in tankyrase inhibitor-treated mice. Thus, it is plausible that the osteoblast-inducing effect of the inhibitor was not exerted in the mice. The findings in radiation chimeric mice lacking tankyrase 1 and 2 in hematopoietic cells, in which tankyrase activity is conserved in the osteoblasts [9], could support this view because the results were similar to our observations in the pharmacological inhibition experiment. Conditional knock-out of tankyrase in osteoblasts will likely be necessary to yield a definitive conclusion on the direct effects of tankyrase inhibition on osteoblastogenesis in vivo.

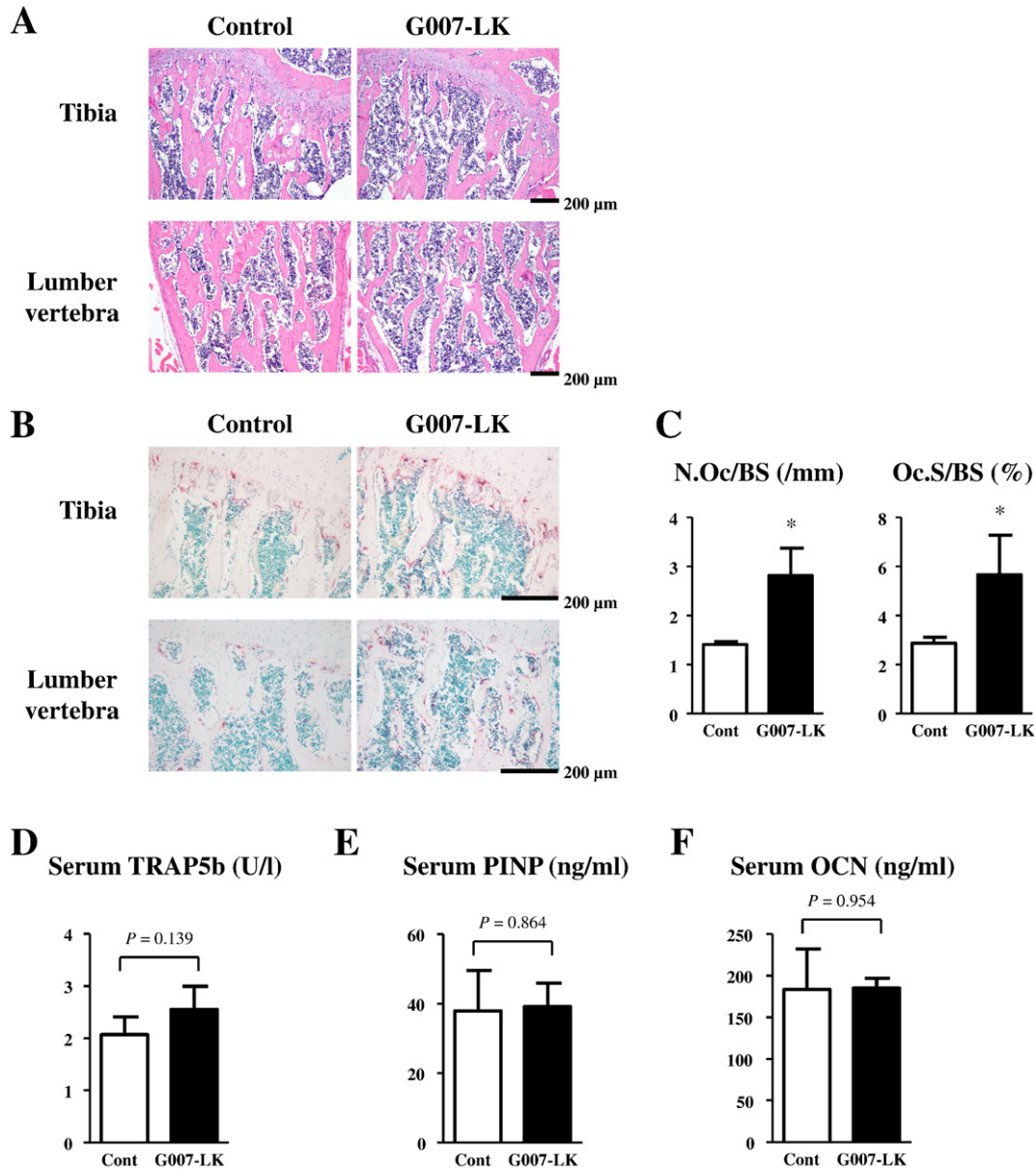


Fig. 7. Increased osteoclast formation in mice by pharmacological tankyrase inhibition. (A) Representative H&E staining images of proximal tibia and lumbar vertebra. (B) Representative TRAP staining images of proximal tibia and lumbar vertebra. (C) Number of osteoclasts per bone surface (N·Oc/BS) and osteoclast surface per bone surface (Oc.S/BS) of proximal tibia were quantitated. (D, E) Levels of serum TRAP5b (D), amino-terminal propeptide of type I procollagen (PINP) (E), and osteocalcin (OCN) (F) were measured by ELISA. Data are presented as means \pm SD. * *P* < 0.05 compared to control mice.

Since tankyrase inhibitors accumulate SH3BP2 protein in macrophages, we should be aware of another possible adverse effect. Macrophages from homozygote SH3BP2 gain-of-function mutant mice exhibit prominent inflammatory responses against Toll-like receptor ligands in an SH3BP2 concentration-dependent manner [15]. Homozygous mice spontaneously develop severe systemic macrophage-rich organ inflammation of the lung, liver, and stomach in addition to a marked osteopenic bone phenotype. To examine whether tankyrase inhibitors affect the response to inflammatory stimuli, RAW264.7 cells were stimulated with lipopolysaccharides in the presence of tankyrase inhibitor. We did not observe any increased inflammatory responses in tankyrase inhibitor-treated RAW264.7 cells (Supp. Fig. 5). Furthermore, the administration of a tankyrase inhibitor to mice did not induce any detectable inflammation-mediated phenotypes, at least at the dose we tested. Although we did not observe activated inflammation in tankyrase inhibitor-treated macrophages and mice, we should consider

the possibility that higher concentrations of tankyrase inhibitors might trigger macrophage-mediated inflammation.

In summary, we uncovered a novel function of tankyrase in osteoclasts and osteoblasts, and revealed that the pharmacological inhibition of tankyrase causes systemic osteopenia due to increased numbers of osteoclasts. These findings highlight the potential adverse effects of tankyrase inhibitors on bone tissue.

Supplementary data to this article can be found online at <https://doi.org/10.1016/j.bone.2017.10.017>.

Acknowledgments

We would like to thank Dr. Y. Matsumoto (Department of Medicine and Clinical Science, Okayama University Graduate School of Medicine, Dentistry and Pharmaceutical Sciences) for some critical suggestions and Dr. Y. Jyu (Department of Health and Sports Sciences, Kawasaki

University of Medical Welfare) for assisting with micro-CT analysis. We are grateful to H. Nakashima, N. Takemasa, N. Obara, Y. Mino, and T. Jinno for their technical assistance. We are also indebted to the staff at the Research center of Kawasaki Medical School. This work was supported by grants from JSPS KAKENHI (15K09540 to TM), The KAWASAKI Foundation for Medical Science and Medical Welfare (SF), The Okayama Medical Foundation (TM), Research Project Grants from Kawasaki Medical School (29G-004 to SF, 28B-46 to TM, and 27B-60 to YM), and the National Institute of Health (R01DE025870 and R21AR070953 to YU).

Authors' roles

Study design: SF, TM, and YM. Study conduct and data collection: SF and TM. Data analysis: SF and TM. Data interpretation: SF, TM, TM, SK, AN, TS, MK, YU, and YM. Drafting the manuscript: SF, TM, and YM. Manuscript approval: all authors. SF, TM, and YM take responsibility for the integrity of the data analysis.

Conflict of interests

SF, TM, TM, SK, AN, and YM have received scholarship donations from AbbVie, Actelion, Astellas, Bristol-Myers, Chugai, Daiichi-Sankyo, Eisai, Eli Lilly, Japan Blood Products Organization, Mitsubishi-Tanabe, Pfizer, Shionogi, Takeda, Teijin, and UCB. TS has received research grants from Asahi Kasei Pharma, Astellas, Daiichi-Sankyo, Taisho Toyama, Takeda, Teijin, and Pfizer, and consulting fees from Daiichi-Sankyo and Takeda.

References

- [1] S. Smith, I. Girit, A. Schmitt, T. de Lange, Tankyrase, a poly(ADP-ribose) polymerase at human telomeres, *Science* 282 (5393) (1998) 1484–1487.
- [2] S.-M.A. Huang, Y.M. Mishina, S. Liu, A. Cheung, F. Stegmeier, G.A. Michaud, O. Charlat, E. Wiellette, Y. Zhang, S. Wiessner, M. Hild, X. Shi, C.J. Wilson, C. Mickanin, V. Myer, A. Fazal, R. Tomlinson, F. Serluca, W. Shao, H. Cheng, M. Shultz, C. Rau, M. Schirle, J. Schlegl, S. Ghidelli, S. Fawell, C. Lu, D. Curtis, M.W. Kirschner, C. Lengauer, P.M. Finan, J.A. Tallarico, T. Bouwmeester, J.A. Porter, A. Bauer, F. Cong, Tankyrase inhibition stabilizes axin and antagonizes Wnt signalling, *Nature* 461 (7264) (2009) 614–620.
- [3] T. Lau, E. Chan, M. Callow, J. Waaler, J. Boggs, R.A. Blake, S. Magnuson, A. Sambrone, M. Schutten, R. Firestein, O. Machon, V. Korinek, E. Choo, D. Diaz, M. Merchant, P. Polakis, D.D. Holsworth, S. Krauss, M. Costa, A novel tankyrase small-molecule inhibitor suppresses APC mutation-driven colorectal tumor growth, *Cancer Res.* 73 (10) (2013) 3132–3144.
- [4] A. Ulsamer, Y. Wei, K.K. Kim, K. Tan, S. Wheeler, Y. Xi, R.S. Thies, H.A. Chapman, Axin pathway activity regulates in vivo pY654-beta-catenin accumulation and pulmonary fibrosis, *J. Biol. Chem.* 287 (7) (2012) 5164–5172.
- [5] A. Distler, L. Deloch, J. Huang, C. Dees, N.Y. Lin, K. Palumbo-Zerr, C. Beyer, A. Weidemann, O. Distler, G. Schett, J.H. Distler, Inactivation of tankyrases reduces experimental fibrosis by inhibiting canonical Wnt signalling, *Ann. Rheum. Dis.* 72 (9) (2013) 1575–1580.
- [6] S. Ren, B.G. Johnson, Y. Kida, C. Ip, K.C. Davidson, S.L. Lin, A. Kobayashi, R.A. Lang, A.K. Hadjantonakis, R.T. Moon, J.S. Duffield, LRP-6 is a coreceptor for multiple fibrogenic signaling pathways in pericytes and myofibroblasts that are inhibited by DKK-1, *Proc. Natl. Acad. Sci. U. S. A.* 110 (4) (2013) 1440–1445.
- [7] D. Tai, K. Wells, J. Arcaroli, C. Vanderbilt, D.L. Aisner, W.A. Messersmith, C.H. Lieu, Targeting the WNT signaling pathway in cancer therapeutics, *Oncologist* 20 (10) (2015) 1189–1198.
- [8] M. Katoh, Molecular genetics and targeted therapy of WNT-related human diseases (review), *Int. J. Mol. Med.* (2017).
- [9] N. Levaot, O. Voityuk, I. Dimitriou, F. Sircoulomb, A. Chandrakumar, M. Deckert, P.M. Krzyzanowski, A. Scotter, S.Q. Gu, S. Janmohamed, F. Cong, P.D. Simoncic, Y. Ueki, J. La Rose, R. Rottapel, Loss of Tankyrase-mediated destruction of 3BP2 is the underlying pathogenic mechanism of cherubism, *Cell* 147 (6) (2011) 1324–1339.
- [10] R. Ren, B.J. Mayer, P. Cicchetti, D. Baltimore, Identification of a ten-amino acid proline-rich SH3 binding site, *Science* 259 (5098) (1993) 1157–1161.
- [11] N. Levaot, P.D. Simoncic, I.D. Dimitriou, A. Scotter, J. La Rose, A.H. Ng, T.L. Willett, C.J. Wang, S. Janmohamed, M. Grynepas, E. Reichenberger, R. Rottapel, 3BP2-deficient mice are osteoporotic with impaired osteoblast and osteoclast functions, *J. Clin. Invest.* 121 (8) (2011) 3244–3257.
- [12] T. Mukai, S. Ishida, R. Ishikawa, T. Yoshitaka, M. Kittaka, R. Gallant, Y.L. Lin, R. Rottapel, M. Brotto, E.J. Reichenberger, Y. Ueki, SH3BP2 Cherubism mutation potentiates TNF-alpha-induced Osteoclastogenesis via NFATc1 and TNF-alpha-mediated inflammatory bone loss, *J. Bone Miner. Res.* 29 (12) (2014) 2618–2635.
- [13] M. Deckert, S. Tartare-Deckert, J. Hernandez, R. Rottapel, A. Altman, Adaptor function for the Syk kinases-interacting protein 3BP2 in IL-2 gene activation, *Immunity* 9 (5) (1998) 595–605.
- [14] T. Hatani, K. Sada, Adaptor protein 3BP2 and cherubism, *Curr. Med. Chem.* 15 (6) (2008) 549–554.
- [15] Y. Ueki, C.Y. Lin, M. Senoo, T. Ebihara, N. Agata, M. Onji, Y. Saheki, T. Kawai, P.M. Mukherjee, E. Reichenberger, B.R. Olsen, Increased myeloid cell responses to M-CSF and RANKL cause bone loss and inflammation in SH3BP2 “cherubism” mice, *Cell* 128 (1) (2007) 71–83.
- [16] T. Mukai, R. Gallant, S. Ishida, M. Kittaka, T. Yoshitaka, D.A. Fox, Y. Morita, K. Nishida, R. Rottapel, Y. Ueki, Loss of SH3 domain-binding protein 2 function suppresses bone destruction in tumor necrosis factor-driven and collagen-induced arthritis in mice, *Arthritis Rheum.* 67 (3) (2015) 656–667.
- [17] E. Hay, E. Laplantine, V. Geoffroy, M. Frain, T. Kohler, R. Muller, P.J. Marie, N-cadherin interacts with axin and LRP5 to negatively regulate Wnt/beta-catenin signaling, osteoblast function, and bone formation, *Mol. Cell. Biol.* 29 (4) (2009) 953–964.
- [18] D. Karasik, F. Rivadeneira, M.L. Johnson, The genetics of bone mass and susceptibility to bone diseases, *Nat. Rev. Rheumatol.* 12 (8) (2016) 496.
- [19] Y. Matsumoto, J. La Rose, O.A. Kent, M.J. Wagner, M. Narimatsu, A.D. Levy, M.H. Omar, J. Tong, J.R. Krieger, E. Riggs, Y. Storozhuk, J. Pasquale, M. Ventura, B. Yeganeh, M. Post, M.F. Moran, M.D. Grynepas, J.L. Wrana, G. Superti-Furga, A.J. Koleske, A.M. Pendergast, R. Rottapel, Reciprocal stabilization of ABL and TAZ regulates osteoblastogenesis through transcription factor RUNX2, *J. Clin. Invest.* 126 (12) (2016) 4482–4496.
- [20] T. Mukai, R. Gallant, S. Ishida, T. Yoshitaka, M. Kittaka, K. Nishida, D.A. Fox, Y. Morita, Y. Ueki, SH3BP2 gain-of-function mutation exacerbates inflammation and bone loss in a murine collagen-induced arthritis model, *PLoS One* 9 (8) (2014).
- [21] K.H. Emami, C. Nguyen, H. Ma, D.H. Kim, K.W. Jeong, M. Eguchi, R.T. Moon, J.L. Teo, H.Y. Kim, S.H. Moon, J.R. Ha, M. Kahn, A small molecule inhibitor of beta-catenin/CREB-binding protein transcription [corrected], *Proc. Natl. Acad. Sci. U. S. A.* 101 (34) (2004) 12682–12687.
- [22] W.N.H. Koek, B.C.J. van der Eerden, R. Alves, M. van Driel, M. Schreuders-Koedam, M.C. Zillikens, J. van Leeuwen, Osteoclastogenic capacity of peripheral blood mononuclear cells is not different between women with and without osteoporosis, *Bone* 95 (2017) 108–114.
- [23] A.D. Bakker, J. Klein-Nulend, Osteoblast isolation from murine calvaria and long bones, *Methods Mol. Biol.* 816 (2012) 19–29.
- [24] S.B. Peters, Y. Wang, R. Serra, Tgfb2 is required in osterix expressing cells for post-natal skeletal development, *Bone* 97 (2017) 54–64.
- [25] Y.I. Ju, T. Sone, K. Ohnaru, H.J. Choi, K.A. Choi, M. Fukunaga, Jump exercise during hindlimb unloading protect against the deterioration of trabecular bone microarchitecture in growing young rats, *Spring* 2 (1) (2013) 35.
- [26] M.L. Bouxsein, S.K. Boyd, B.A. Christiansen, R.E. Goldberg, K.J. Jepsen, R. Muller, Guidelines for assessment of bone microstructure in rodents using micro-computed tomography, *J. Bone Miner. Res.* 25 (7) (2010) 1468–1486.
- [27] D.W. Dempster, J.E. Compston, M.K. Drezner, F.H. Glorieux, J.A. Kanis, H. Malluche, P.J. Meunier, S.M. Ott, R.R. Recker, A.M. Parfitt, Standardized nomenclature, symbols, and units for bone histomorphometry: a 2012 update of the report of the ASBMR Histomorphometry nomenclature committee, *J. Bone Miner. Res.* 28 (1) (2013) 2–17.
- [28] L. Lehtio, N.W. Chi, S. Krauss, Tankyrases as drug targets, *FEBS J.* 280 (15) (2013) 3576–3593.
- [29] T. Nakashima, M. Hayashi, H. Takayanagi, New insights into osteoclastogenic signaling mechanisms, *Trends Endocrinol. Metab.* 23 (11) (2012) 582–590.
- [30] Y. Muramatsu, T. Ohishi, M. Sakamoto, T. Tsuruo, H. Seimiya, Cross-species difference in telomeric function of tankyrase 1, *Cancer Sci.* 98 (6) (2007) 850–857.
- [31] J.A. Ledermann, P. Harter, C. Gourley, M. Friedlander, I. Vergote, G. Rustin, C. Scott, W. Meier, R. Shapira-Frommer, T. Saif, D. Matei, A. Fielding, S. Spencer, P. Rowe, E. Lowe, D. Hodgson, M.A. Sovak, U. Matulonis, Overall survival in patients with platinum-sensitive recurrent serous ovarian cancer receiving olaparib maintenance monotherapy: an updated analysis from a randomised, placebo-controlled, double-blind, phase 2 trial, *Lancet Oncol.* 17 (11) (2016) 1579–1589.
- [32] M. Robson, S.A. Im, E. Senkus, B. Xu, S.M. Domchek, N. Masuda, S. Delalogue, W. Li, N. Tung, A. Armstrong, W. Wu, C. Goessl, S. Runswick, P. Conte, Olaparib for metastatic breast cancer in patients with a germline BRCA mutation, *N. Engl. J. Med.* 377 (6) (2017) 523–533.
- [33] B. Li, S. Boast, K. de los Santos, I. Schieren, M. Quiroz, S.L. Teitelbaum, M.M. Tondravi, S.P. Goff, Mice deficient in Abl are osteoporotic and have defects in osteoblast maturation, *Nat. Genet.* 24 (3) (2000) 304–308.
- [34] Y.J. Chiang, S.J. Hsiao, D. Yver, S.W. Cushman, L. Tassarollo, S. Smith, R.J. Hodes, Tankyrase 1 and tankyrase 2 are essential but redundant for mouse embryonic development, *PLoS One* 3 (7) (2008), e2639.
- [35] E.J. Reichenberger, M.A. Levine, B.R. Olsen, M.E. Papadaki, S.A. Lietman, The role of SH3BP2 in the pathophysiology of cherubism, *Orphanet J. Rare Dis.* 7 (Suppl. 1) (2012) S5.
- [36] M.E. Papadaki, S.A. Lietman, M.A. Levine, B.R. Olsen, L.B. Kaban, E.J. Reichenberger, Cherubism: best clinical practice, *Orphanet J. Rare Dis.* 7 (Suppl. 1) (2012) S6.
- [37] Y. Ueki, V. Tiziani, C. Santanna, N. Fukai, C. Maulik, J. Garfinkle, C. Ninomiya, C. doAmaral, H. Peters, M. Habal, L. Rhee-Morris, J.B. Doss, S. Kreiberg, B.R. Olsen, E. Reichenberger, Mutations in the gene encoding c-Abl-binding protein SH3BP2 cause cherubism, *Nat. Genet.* 28 (2) (2001) 125–126.
- [38] H. Gunaydin, Y. Gu, X. Huang, Novel binding mode of a potent and selective tankyrase inhibitor, *PLoS One* 7 (3) (2012), e33740.
- [39] O. Arques, I. Chicote, I. Puig, S.P. Tenbaum, G. Argiles, R. Dienstmann, N. Fernandez, G. Caratu, J. Matito, D. Silberschmidt, J. Rodon, S. Landolfi, A. Prat, E. Espin, R. Charco, P. Nuciforo, A. Vivancos, W. Shao, J. Taberner, H.G. Palmer, Tankyrase inhibition blocks Wnt/beta-catenin pathway and reverts resistance to PI3K and AKT inhibitors in the treatment of colorectal cancer, *Clin. Cancer Res.* 22 (3) (2016) 644–656.
- [40] H. Seimiya, Y. Muramatsu, T. Ohishi, T. Tsuruo, Tankyrase 1 as a target for telomere-directed molecular cancer therapeutics, *Cancer Cell* 7 (1) (2005) 25–37.